

Implementation of Joint Pre-FFT Adaptive Array Antenna and Post-FFT Space Diversity Combining for Mobile ISDB-T Receiver

Dang Hai PHAM^{†,††a)}, Jing GAO[†], Takanobu TABATA^{†††}, Hirokazu ASATO^{††}, *Nonmembers*, Satoshi HORI^{†††},
and Tomohisha WADA^{†,††}, *Members*

SUMMARY In our application targeted here, four on-glass antenna elements are set in an automobile to improve the reception quality of mobile ISDB-T receiver. With regard to the directional characteristics of each antenna, we propose and implement a joint Pre-FFT adaptive array antenna and Post-FFT space diversity combining (AAA-SDC) scheme for mobile ISDB-T receiver. By applying a joint hardware and software approach, a flexible platform is realized in which several system configuration schemes can be supported; the receiver can be reconfigured on the fly. Simulation results show that the AAA-SDC scheme drastically improves the performance of mobile ISDB-T receiver, especially in the region of large Doppler shift. The experimental results from a field test also confirm that the proposed AAA-SDC scheme successfully achieves an outstanding reception rate up to 100% while moving at the speed of 80km/h.

key words: adaptive array antenna, space diversity combining, OFDM, ISDB-T, FPGA, DSP

1. Introduction

Terrestrial Integrated Services Digital Broadcasting (ISDB-T) as digital TV broadcasting service in Japan started to launch nationwide from 2006. Orthogonal Frequency Division Multiplexing (OFDM), also referred to as a multi-carrier modulation scheme, is adopted as a modulation method of ISDB-T standard. OFDM is well-known as a high-spectral efficiency transmission method in the multipath environment [1], [2]. However, ISDB-T standard mainly aims to fully support fixed reception applications. In a circumstance that OFDM receiver is set on the automobile, orthogonality among OFDM subcarrier is destroyed due to Doppler shift as the automobile is moving. Therefore, it is a severe challenge to maintain the reception quality of mobile ISDB-T receiver at a certain level that is acceptable for human vision.

One well-known way to improve the performance of OFDM receiver is to exploit a spatial diversity by utilizing multiple antenna elements. Typically, depending on whether the Fast Fourier transform (FFT) is performed before or after diversity combining, the structure of an OFDM receiver

is then classified into two types: Pre-FFT scheme and Post-FFT scheme. In Pre-FFT scheme, array antenna utilizes digital beam-forming (DBF) algorithm to form beam toward the desired signal [3], [4]. Since this approach only relates to processes prior to FFT, it is an attractive solution in term of low computation requirement. Several approaches based on adaptive array antenna and Pre-FFT scheme, namely as Pre-FFT adaptive array antenna (Pre-FFT AAA) scheme, have been proposed to improve the performance of mobile OFDM receiver in multipath condition [5]–[10]. In our previous works [11] and [12], we proposed and implemented the Pre-FFT AAA scheme, in which several DBF algorithms have been adopted, such as Maximum Ratio Combining (MRC), Adaptively Main Beam Forming (AMBF) as the improvement algorithm of MRC, and Sample Matrix Inversion (SMI). On the other hand, Post-FFT scheme is an optimum approach in term of maximizing signal-to-noise ratio (SNR) for each OFDM subcarriers [13]–[15]. However, its computation complexity grows drastically as more antenna elements associated with equivalent OFDM demodulations are used.

In this paper, we propose a joint Pre-FFT adaptive array antenna and Post-FFT space diversity combining scheme, hereto referred to as AAA-SDC, as a trade-off approach to improve the performance of mobile ISDB-T receiver with reasonable requirement of computation complexity. For our particular application, four on-glass antenna elements are set in the body of automobile. Interestingly, as the body of automobile is made from metal, one should take into account the fact that the directional characteristic of antenna element is distorted and seemingly concentrates on the outside of the automobile [17]. To exploit the unique property of on-glass antenna elements, we also propose the implementation of the AAA-SDC scheme for mobile ISDB-T receiver, in which several implementation-related issues is dealt with, e.g. Doppler shift, frequency error, sampling rate error and timing synchronization. The target of our design is not only to improve the reception quality but also to provide the flexible and unified platform that is capable of reconfiguration and further improvement. The performance of the proposed scheme is evaluated by simulation and the prototype is validated in field experiments.

The rest of the paper is organized as follows. In the next section, signal models of the proposed AAA-SDC scheme and DBF algorithms such as MRC, AMBF and SMI are introduced. In Sect. 3, issues related to implementations

Manuscript received May 8, 2007.

Manuscript revised July 20, 2007.

[†]The authors are with the Faculty of Engineering, Dept. of Information Engineering, Univ. of the Ryukyus, Okinawa-ken, 903-0213 Japan.

^{††}The authors are with Magna Design Net Inc., Naha-shi, 901-0152 Japan.

^{†††}The authors are with Kojima Press Industry Co., Ltd., Aichi-ken, 470-0207 Japan.

a) E-mail: phdang@lsi.ie.u-ryukyu.ac.jp

DOI: 10.1093/ietcom/e91-b.1.127

of the proposed AAA-SDC scheme for our application are discussed. The implementation of the AAA-SDC scheme is verified by simulations and experiments, the results are provided in Sect. 4 and Sect. 5. Finally, conclusions are given in Sect. 6.

2. OFDM Signal Model

In OFDM transmitter, data stream is serial-to-parallel divided into multiple substreams modulated by inverse fast Fourier transform (IFFT). Then, GI (Guard Interval) is inserted at the output of IFFT. The OFDM transmitted base-band signal can be expressed as

$$s(n) = \frac{1}{\sqrt{N_c}} \sum_{k=-N_c/2}^{N_c/2-1} a(i, k) e^{j2\pi \frac{nk}{N_c}} \quad (1)$$

where $a(i, k)$ denotes a complex modulation data of k -th subcarrier of i -th OFDM symbol and N_c denotes the number of OFDM subcarriers.

The OFDM received signal via multipath channel is derived as follow

$$y(n) = h(n) \otimes s(n) + \eta(n) \quad (2)$$

where \otimes denotes the convolution. $h(n)$ and $\eta(n)$ are channel impulse response (CIR) of multipath channel and additive noise, respectively.

At the receiver, after removing GI, the received signal is demodulated by using the FFT. The OFDM received symbol at k -th subcarrier of i -th OFDM symbol is derived as

$$Y(i, k) = \sum_{n=0}^{N_c-1} y(n) e^{-j2\pi \frac{nk}{N_c}} \quad (3)$$

$$= H(i, k) a(i, k) + N(i, k)$$

where $H(i, k)$ and $N(i, k)$ are channel transfer function (CTF) and additive noise at k -th subcarrier of i -th OFDM symbol, respectively.

$$H(i, k) = \sum_{n=0}^{N_c-1} h(n) e^{-j2\pi \frac{nk}{N_c}} \quad (4)$$

$$N(i, k) = \sum_{n=0}^{N_c-1} \eta(n) e^{-j2\pi \frac{nk}{N_c}}$$

2.1 Pre-FFT Adaptive Array Antenna

DBF algorithms that exploit the periodic property of OFDM signal are realized. OFDM signal is comprised of GI with duration of T_g and an effective symbol with duration of T_e . Indeed, GI is a copy from the last part of the effective symbol. In this paper, GI is referred to as “HeadGI” in order to distinguish from the original part, which is referred to as “TailGI.”

Figure 1 illustrates the principle of the Pre-FFT AAA scheme [12]. Suppose that a linear array antenna is equipped

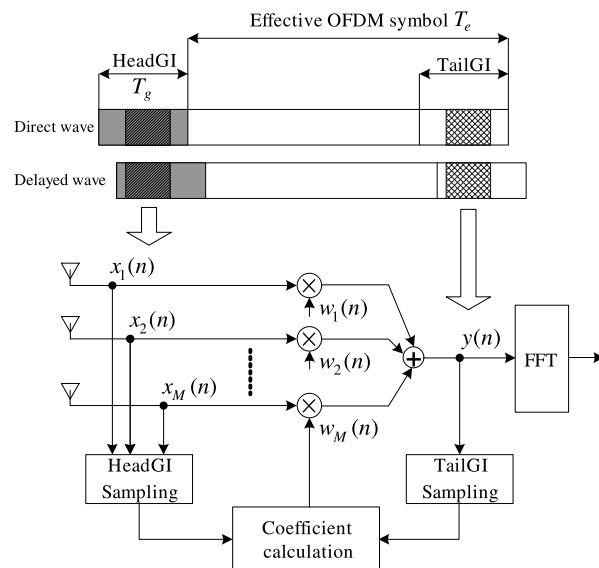


Fig. 1 The principle of the Pre-FFT AAA scheme.

with M element antenna. Thus, an input vector of the AAA scheme is expressed as

$$\mathbf{X}(n) = [x_1(n) \quad x_2(n) \quad \dots \quad x_M(n)]^T \quad (5)$$

Hence, the output of the AAA scheme is calculated as follows

$$y(n) = \mathbf{W}^H \mathbf{X}(n) \quad (6)$$

where superscripts $(\cdot)^T$ and $(\cdot)^H$ denote the transpose and the conjugate transpose, respectively.

$\mathbf{W} = [w_1 \quad w_2 \quad \dots \quad w_M]^T$ is a coefficient vector of the AAA scheme.

In our previous work [12], DBF algorithms were investigated and implemented. Again, they are adopted for the Pre-FFT scheme and their signal models are briefly given in the following.

Firstly, MRC algorithm is recursively derived from the cross-correlation of inputs and output of the Pre-FFT AAA scheme [12]. Accordingly, the initial coefficients of the Pre-FFT AAA is set so that the input of only one antenna is used as the output. Then, the coefficients of MRC algorithm is recursively determined for next OFDM symbol and is expressed as

$$\mathbf{W}_{MRC} = E [\mathbf{X}(n) y^*(n)] \quad (7)$$

where $E[\cdot]$ denotes the expectation function.

Secondly, AMBF, which is based on MRC algorithms, is derived in order to exploit the periodic property of OFDM signal. Hence, the coefficients of AMBF algorithm are derived from the cross-correlation of HeadGIs of inputs and TailGI of output as follows

$$\mathbf{W}_{AMBF} = E [\mathbf{X}_h(n) y_t^*(n)] \quad (8)$$

where $\mathbf{X}_h(n)$ denotes HeadGIs of input vector, $y_t(n)$ denotes

TailGI of output.

Finally, SMI algorithm is also adopted for the Pre-FFT AAA scheme. Instead of forming the beams toward the strongest path, SMI algorithm steers nulls toward DOAs (Direction-Of-Arrival) of interferences. The coefficients of SMI are given as

$$\mathbf{W}_{SMI} = \mathbf{R}_{xx}^{-1} \mathbf{W}_{AMBF} \quad (9)$$

where $\mathbf{R}_{xx} = E[\mathbf{X}_h \mathbf{X}_h^H]$ is auto correlation matrix of inputs.

2.2 Post-FFT Space Diversity Combining

Figure 2 illustrates the principle of the Post-FFT SDC in the OFDM receiver. Suppose that the Post-FFT SDC consists of M FFTs corresponding to M OFDM demodulators. The combined symbol at k -th subcarrier of i -th OFDM symbol is given as follows

$$Z(i, k) = \sum_{l=1}^M C_l(i, k) Y_l(i, k) \quad (10)$$

where $C_l(i, k)$ and $Y_l(i, k)$ are combining coefficient and received symbol corresponding to l -th branch of Post-FFT SDC at k -th subcarrier of i -th OFDM symbol, respectively.

Assume that each subcarrier suffers the flat fading condition due to its narrow bandwidth and the perfect CTF estimation is also utilized. Thus the combining coefficient corresponding to l -th branch of the Post-FFT SDC at k -th subcarrier can be derived by using the MRC algorithm as follows [14]

$$C(i, k) = \frac{H_l^*(i, k)}{\sum_{l=1}^M |H_l(i, k)|^2} \quad (11)$$

where $H_l(i, k)$ is CTF of l -th branch at k -th subcarrier of i -th OFDM symbol.

By using MRC algorithm, the optimum SNR can be achieved for each subcarrier in the Post-FFT SDC scheme [24].

2.3 Proposed Joint Pre-FFT Adaptive Array Antenna and Post-FFT Space Diversity Combining

The Post-FFT SDC scheme mentioned above is literally an optimum solution to achieve the maximum diversity gain with given antenna elements. However, due to a very high computation complexity, recently, the implementation of the Post-FFT SDC scheme is usually comprised of up to four OFDM demodulations.

In this paper, we propose a joint Pre-FFT adaptive array antenna and Post-FFT space diversity combining scheme for OFDM receiver, named as the AAA-SDC scheme. Hence, the AAA-SDC scheme can be considered as a trade-off solution to achieve a reasonable diversity gain with a relatively low computation complexity.

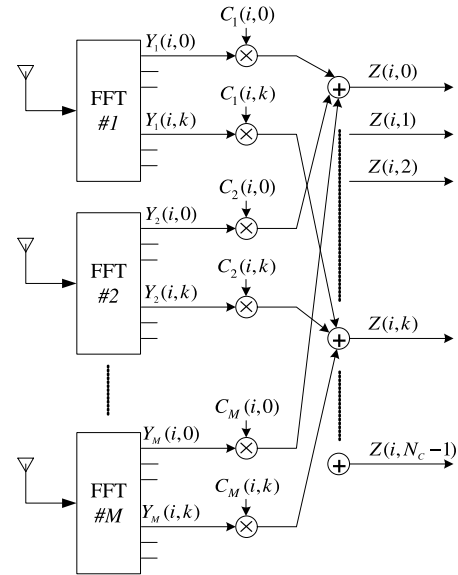


Fig. 2 The principle of the space diversity combining scheme (SDC) of OFDM receiver.

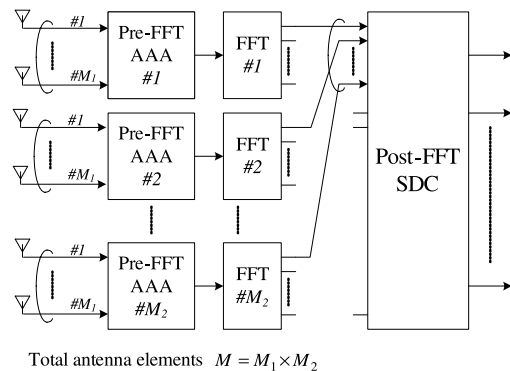


Fig. 3 The proposed joint Pre-FFT adaptive array antenna and post-FFT space diversity combining of OFDM receiver.

Figure 3 illustrates the principle of the proposed AAA-SDC scheme. The proposed AAA-SDC scheme is comprised of M_2 Pre-FFT AAA schemes corresponding to M_2 OFDM demodulations of the Post-FFT SDC scheme. Each Pre-FFT AAA scheme is comprised of M_1 antenna elements. It is worthwhile to note that the total number of antenna elements is kept unchanged, i.e. $M = M_1 \times M_2$. Several DBF algorithms, e.g. MRC, AMBF and SMI, are performed in the Pre-FFT AAA scheme as discussed in Sect. 2.1. Outputs of them are fed to the Post-FFT SDC scheme to perform diversity combining for each subcarrier of OFDM symbols as discussed in Sect. 2.2.

Next, the implementation of the proposed AAA-SDC scheme for mobile ISDB-T receiver is discussed. Additionally, implementation-related issues that greatly impact on the performance of the proposed scheme are also dealt with in the next section.

3. Implementation of the Proposed AAA-SDC Scheme for Mobile ISDB-T Receiver

In this section, the implementation of the proposed AAA-SDC scheme is discussed from the viewpoint of hardware design. The target of our design is to improve the performance of the mobile ISDB-T receiver up to a certain level of reception quality. It is also required to provide a flexible and unified platform that is capable of reconfigurations and further improvements.

3.1 Implementation-Related Issues

As realizing the AAA-SDC scheme, several implementation related issues are brought to our concern and listed as follows

- Doppler shift and frequency error due to imperfect oscillator.
- Sampling rate error due to the mismatch sampling frequency between the transmitter and the receiver.
- OFDM symbol synchronization and CTF estimation.

Next, these issues are discussed thoroughly and their treatments are summarized.

A. Doppler Shift and Frequency Error.

In mobile ISDB-T receiver, incoming signal with carrier frequency of f_c comes to antenna with angle-of-arrival (AOA) of θ . As a result, each subcarrier of the OFDM signal suffers a Doppler shift as

$$\begin{aligned} f_d &= \frac{v}{c} f_c \cos(\theta) \\ &= \frac{v}{\lambda} \cos(\theta) \end{aligned} \quad (12)$$

where λ is wavelength of incoming signal; v and c are the speed of the automobile and the light, respectively. The maximum Doppler shift is determined as $f_{d\max} = (v/c)f_c$.

In mobile channel, assume that many waves arrive each with its own random AOA (thus with its own Doppler shift), which is uniformly distributed within $[0, 2\pi]$, independently of other waves. A probability density function of the frequency of received signal can be obtained, referred to as Doppler spectrum [24]. Figure 4(a) illustrates Doppler spectrum of received signal associated with an omnidirectional antenna, i.e. all frequency components of received signal are subjects of Doppler shift randomly distributed within $[-f_{d\max}, +f_{d\max}]$.

In our application, totally four antenna elements are utilized and are set in the body of automobile, two antenna elements are set in the front and the others are set in the rear. However, as the body of automobile is made from metal, two front antenna elements seemingly experience a similar Doppler shift as discussed below, so do the others in the rear. Hence, in order to simply demonstrate different Doppler

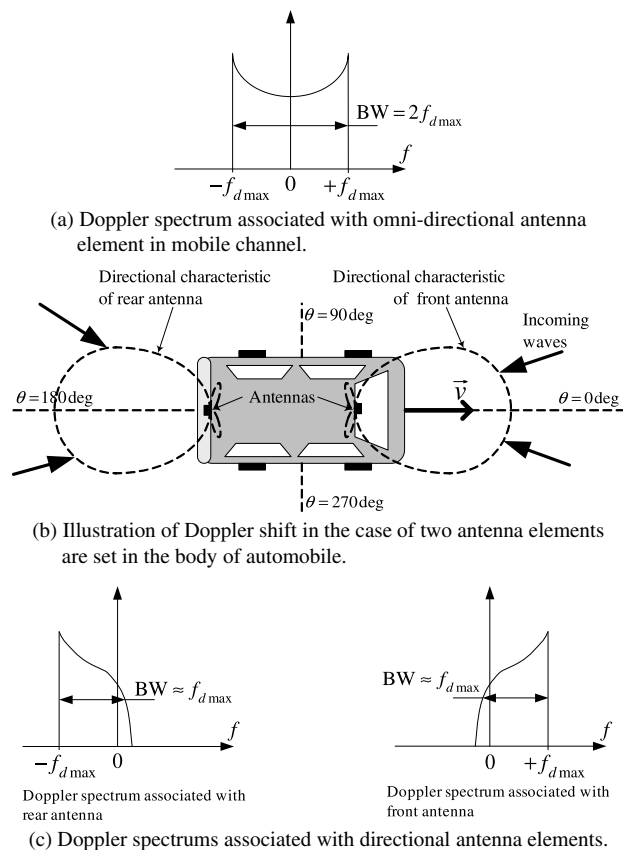


Fig. 4 Illustration of Doppler effect in case antenna elements are set in the body of automobile.

shift phenomenon between the front and rear antenna elements, let us assume in this subsection that there are only two antenna elements, one set in the front and the other set in the rear of the body of automobile — see Fig. 4(b). As the body of automobile is made from metal, it is experimentally confirmed that directional characteristic of the front antenna is obviously distorted and concentrates on the front direction, while that of the rear antenna focuses to the back direction of automobile [17]. Therefore, these antenna elements can be considered as direction filters of which AOA of incoming signal is the subject. Consequentially, as illustrated in Fig. 4(c), received signal of front antenna element mostly experiences a *positive* Doppler shift randomly distributed within $[0, +f_{d\max}]$; whereas that of rear antenna element mostly experiences a *negative* Doppler shift randomly distributed within $[-f_{d\max}, 0]$. In other words, performance of mobile ISDB-T receiver is seemingly enhanced in mobile channel condition as bandwidth of Doppler spectrum is reduced by exploiting directional antenna elements.

In addition, imperfect analog components, such as carrier frequency oscillator, also introduce a frequency error to the received signal. A frequency error caused by imperfect analog components can be considered to be invariant in duration of many OFDM symbols. As a result, ICI (Inter-carrier Interference) caused by both Doppler shift and imperfect analog components will increase the error floor of re-

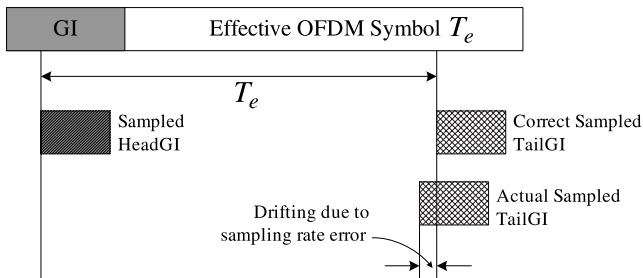


Fig. 5 Impact of sampling rate error.

ceived symbol at each subcarrier. Therefore, it is important to cope with the *total frequency error* caused by Doppler shift and imperfect analog components. Moreover, in our specific application, frequency error of the front antenna and that of the rear antenna should be estimated and compensated separately due to their opposite Doppler shifts. The methodology to cope with frequency error for our application is discussed thoroughly in Sect. 3.2. It is worthwhile to note that the accuracy of frequency error estimation can be enhanced by exploiting directional antenna elements.

B. Sampling Rate Error.

The mismatch of sampling rate between a transmitter and a receiver is unavoidable in a wireless communication system. Figure 5 illustrates an impact of sampling rate error on a sampled TailGI. Due to the drifting of sampling positions of TailGI, the cross correlation between HeadGI of inputs and TailGI of the output is severely deteriorated. Therefore, it is important to cope with sampling rate error in order to improve performances of DBF algorithms in reality.

Decimation/interpolation as a digitally timing-adjustment process is a well-known method to cope with sampling error and is covered extensively in the literature [22], [23]. Moreover, in our system, the sampling rate of received OFDM signals is always slightly higher than that of transmitted signals. The purpose of that is to simplify the decimation/interpolation process, i.e. only interpolation process is necessary to compensate sampling rate error, consequently.

C. Timing Synchronization Error.

Due to the nature of wireless communication, timing synchronization error is inevitable. In our design, the performance of DBF algorithms are greatly impacted by the accurate timing synchronization as sampling HeadGIs and TailGIs. In addition, the performance of CTF estimation is essential for Post-FFT diversity combining scheme.

These errors mentioned above are issues one should carefully deal with in order to enhance the robustness of the AAA-SDC scheme. In [20], OFDM signal model with the presence of these errors is investigated. In [21] the optimum structure of OFDM receiver are proposed, in which error estimation processes are realized both prior and after

FFT. In our design, a joint symbol synchronization and frequency error compensation are realized based on the periodic property of OFDM signal [19]. Additionally, as the ISDB-T standard employs scattered pilots (SPs) in subcarriers, CTF can be estimated by performing 2D interpolation on SPs. Estimations of CIR and a delay profile of multipath channel can also be obtained by performing IFFT on CTF. In our circumstance, by monitoring the position of the peak of the delay profile, sampling rate error and precise timing synchronization are estimated and compensated prior to FFT. In Sect. 3.2, the functional block diagram for hardware implementation is disclosed and discussed thoroughly.

3.2 Implementation of the AAA-SDC OFDM Receiver

In this subsection, the implementation of the AAA-SDC scheme for mobile OFDM receiver is discussed. Again, one should keep in mind that the application of the mobile OFDM receiver is specifically to be set in the automobile. Due to the limitation on the automobile's space and, more importantly, the cost of hardware complexity, four antenna elements are employed, of which two antenna elements are set in the front and the others are set in the rear of the automobile.

Figure 6 shows the block diagram of the AAA-SDC scheme for mobile OFDM receiver. Received signals from four antenna elements are down-converted and analog-to-digital converted. It is important to mention here that:

- Received signals from antenna elements experience similar sampling rate error because the common carrier frequency oscillator is used.
- Doppler shift and timing synchronization error are similar for received signal from either front antenna elements or rear ones due to the close distance of them.
- However, Doppler shift and timing synchronization error are seemingly independent from front antenna elements to rear ones due to the distant separation of them and the material of automobile's body.

In our implementation, the estimation processes, such as sampling rate error estimation, frequency error estimation and timing synchronization estimation, are utilized before and after FFT transformation, namely Pre-FFT and Post-FFT estimations [19], [20].

After compensating the sampling rate error and frequency error, HeadGI of received signals and TailGI of the combined signals from the array antenna are sampled and stored into memory BRAM. The DSP is responsible for generating the coefficients of the AAA. There are two independent OFDM demodulations corresponding to two branches of the SDC scheme. Each branch is comprised of FFT and CTF estimation. The output signal of the SDC is fed to the FEC (Forward Error Correction) to obtain data stream. Note that implementation of the AAA-SDC scheme associates with several system configuration parameters, such as AAA_opt and SDC_opt as configuration parameters of Pre-FFT AAA scheme and Post-FFT SDC scheme respectively.

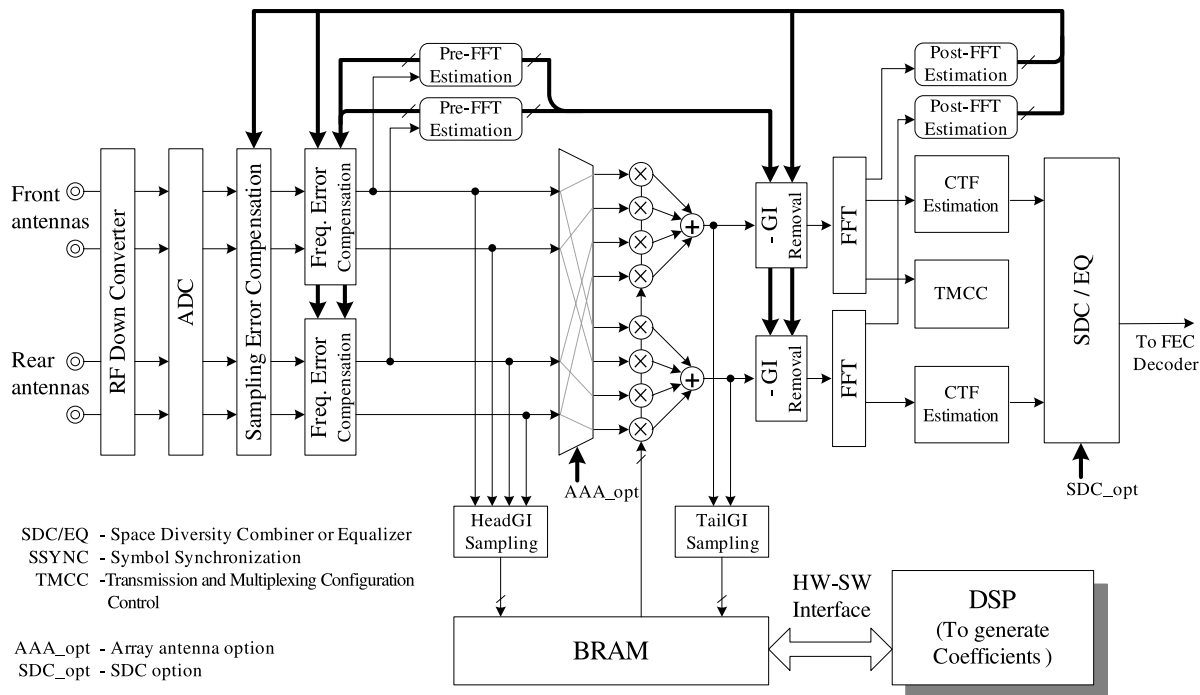


Fig. 6 Block diagram of the proposed AAA-SDC scheme.

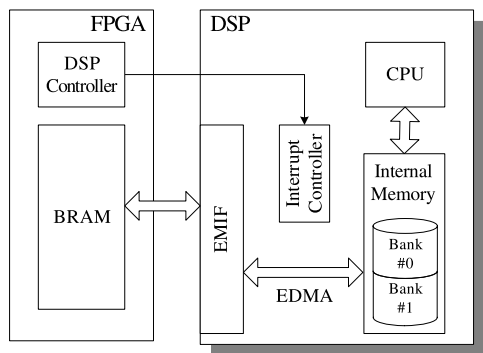


Fig. 7 Interface between FPGA and DSP.

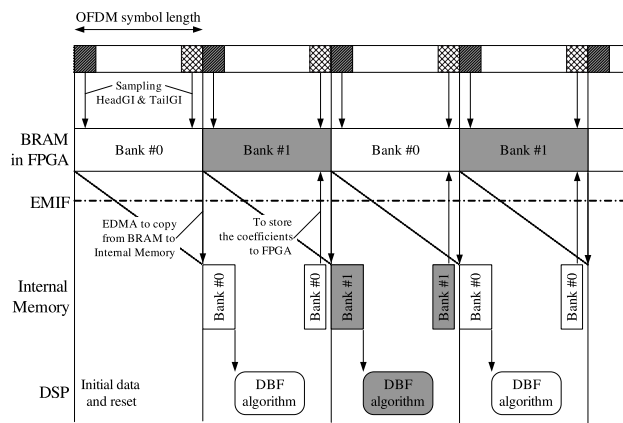


Fig. 8 Timing diagram the AAA-SDC scheme.

Their features are explained in next subsections.

A. Joint Hardware and Software Implementation.

We use joint hardware and software approach for implementing the proposed AAA-SDC scheme — see Fig. 6. FPGA is utilized as hardware side due to its million-logic-gate density and gigabit-per-second interface. Therefore prefixed processes which also demand high computation load, such as FFTs, CTF estimation, Pre-FFT and Post-FFT estimations, are synthesized in FPGA. In contrast, DBF algorithms that require less computation load are realized in DSP. In our design, TI C6713 development board is used to perform DBF algorithms. It features the TMS320C6713 DSP of 225 MHz with floating-point support, which meets the demand of high precision computation for DBF algorithms. This joint hardware and software approach surely

provide a robust platform for investigation and further improvement. Figure 7 shows the interface of FPGA and DSP. FPGA and DSP are coupled via a shared memory block located in FPGA, namely BRAM. BRAM is a dual-port memory block which provides a common memory accessible to both FPGA and DSP that can be used to share and transmit data and system status between them. DSP retrieves data in BRAM via EMIF (External Memory Interface) using EDMA (Enhanced Direct-Memory-Access). Handshake signal from FPGA is used as external interrupt to trigger the data transfer process and the operation of CPU.

In detail, a dual memory bank is utilized in both BRAM and internal memory of DSP to realize real-time operation. Timing diagram is illustrated in Fig. 8. As mentioned above, BRAM provides common memory accessible to both

Table 1 Specification of the prototype.

Adaptive Array Antenna	ADC	Channel	4
		Resolution	10 bit
		Sampling rate	32 MHz
Space Diversity Combining	FPGA	Xilinx Virtex-II Pro VP70, VP20	
	DSP	TI DSP C6713 TMS320C6713 225 MHz	
Space Diversity Combining	FPGA	Xilinx Virtex-II 4000x2, V3000 (OFDM Demod. and SDC)	

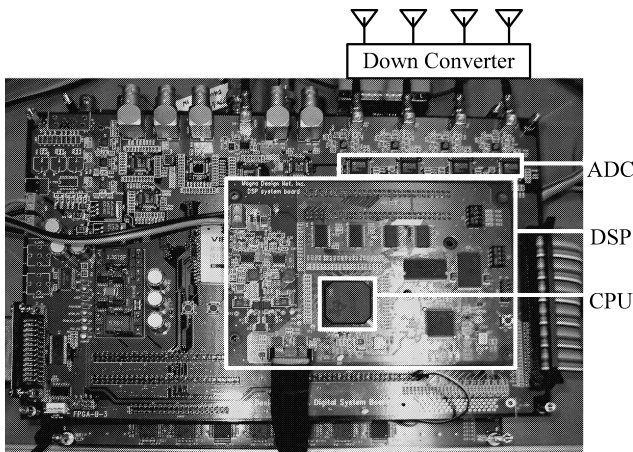


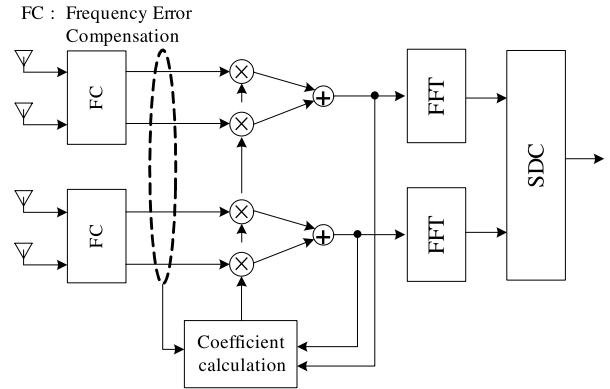
Fig. 9 Prototype of the AAA-SDC scheme.

FPGA and DSP. In FPGA, samples of HeadGI and TailGI are stored continuously to bank #0 and bank #1 in BRAM. Meanwhile, DSP retrieves data samples available in one memory bank in BRAM to generate the coefficients. After that, the coefficients are stored back to the corresponding memory bank in BRAM. The duration for retrieving data samples, generating the coefficients and storing the coefficients is shorter than one OFDM symbol duration.

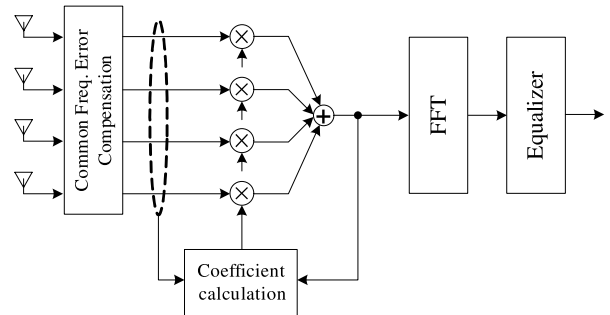
We successfully implement the prototype of the AAA-SDC scheme. Table 1 and Fig.9 show the specification and photograph of a prototype of the proposed AAA-SDC scheme.

B. Multiple System Configurations featured by the AAA-SDC Scheme.

The prototype is capable of altering the combination of antenna elements, i.e. four antenna elements can be used as one array antenna or as two array antenna, of which one is set in the front and the other is set in the rear of automobile. In addition, the operation of the Post-FFT SDC scheme can also be switched to a conventional equalizer by using only one OFDM demodulation. As a result, the prototype can be utilized as the proposed AAA-SDC scheme or as the Pre-FFT AAA scheme. Nevertheless, since DBF algorithms are embedded in DSP, beam-forming capability of the array antenna can also be reconfigurable on the fly. The capabilities of reconfiguring the system configuration and changing dif-



(a) System configuration A as the proposed joint AAA-SDC scheme.



(b) System configuration B as the conventional Pre-FFT AAA scheme.

Fig. 10 Multiple system configurations supported by the AAA-SDC scheme.

ferent DBF algorithms are to flexibly adapt the design for various applications. We believe these features are useful for investigation and further improvement.

Two system configurations are featured for evaluation and experiment. Figure 10(a) shows the proposed AAA-SDC scheme as a fully supported system configuration, in which both Pre-FFT AAA scheme and Post-FFT SDC scheme are exploited, and is hereto referred to as *System Configuration A*. The other, shown in Fig. 10(b), is the conventional Pre-FFT AAA scheme referred to as *System Configuration B* [12]. Their implementations are significantly different, such as:

- System Configuration A aims to exploit capabilities of beam forming and diversity combining algorithm with regard to directional characteristics of antenna elements set in automobile. Meanwhile, System Configuration B only supports beam forming capability.
- In System Configuration A, two independent frequency error compensations are used for received signals from two front antennas and two rear antennas. However, in System Configuration B, only common frequency error compensation is used.

The performances of the prototype with both system configurations are evaluated by simulations and field experiments comparatively and the results are given in Sect. 4 and Sect. 5.

4. Simulation Results

In this section, the operation of the AAA-SDC scheme is verified and studied by simulation. Coware Signal Processing Worksystem (SPW) is used as a developing EDA tool. SPW provides a flexible visualization environment with block-oriented design. Nevertheless, because of its capability of co-simulating multiple languages, such as VHDL, Verilog HDL as well as C/C++, ones can possibly perform the system-level design in a single design workbench in order to verify the operation in co-simulating environment straightforwardly.

To evaluate performance of the AAA-SDC scheme in our application, based on [16], directional characteristics of antenna elements are modeled as

$$E(\theta) = \begin{cases} E_0 \cos [k(\theta - \theta_0)], & k|\theta - \theta_0| \leq 90^\circ \\ & \text{or } k(|\theta - \theta_0| - 360^\circ) \geq -90^\circ \\ 0 & \text{otherwise} \end{cases} \quad (13)$$

where $E(\theta)$ is an electric field strength in direction of θ , E_0 is the maximum electric field strength of the antenna element. θ_0 is center direction of each antenna element and k is a beam width parameter.

In this paper, the value of k is determined by given beam width in which the electric field strength remains larger than a half of E_0 , referred to as half-power beam width (HPBW). Thus, HPBW and the center direction of each antenna element could be used to model antenna directional characteristic in these evaluations hereafter.

Table 2 shows the specifications of the AAA-SDC scheme. Furthermore, Fig. 11 illustrates electrical field strength of antenna elements. As such, front antenna #1 and #2 with HPBW of 120 deg and center directions of 30 deg and 330 deg, respectively, essentially concentrate their directional characteristics on the front direction of the automobile. In contrast, rear antenna #1 and #2 with HPBW of 120 deg and center directions of 150 deg and 210 deg mainly concentrate on the back direction of automobile. Mode3 of ISDB-T standard using 64 QAM modulation scheme and GI

Table 2 Specification of the AAA-SDC scheme.

Two 2-antenna element linear arrays		
	Center direction	Distant
Front 1	30 deg	Half-wavelength = 0.2662 m
Front 2	330 deg	
Rear 1	150 deg	Half-wavelength = 0.2662 m
Rear 2	210 deg	
HPBW=120 deg		
ISDB-T using DTV28CH Mode3		
Carrier Frequency	563.143 MHz	
FFT size	8192	
Number of Subcarrier	5617	
Effective Sym. Duration T_e	1008 μ s	
GI duration $T_g = T_e/8$	126 μ s	
Modulation	64 QAM	

duration $T_e = T_g/8$ is selected as the simulation condition. In order to simplify the verification of the proposed AAA-SDC scheme, a perfect frequency error estimation is used. Also keep in mind that BER measurements are undertaken without Viterbi decoder.

As mentioned in Sect. 3, several system configurations can be supported by using configuration parameters. In the previous project [11], [12], the Pre-FFT array antenna has been implemented due to its lowest cost in computation complexity. Therefore, in order to demonstrate the continuous progress of our project and to convey the viewpoint of hardware design, the performance of the proposed AAA-SDC scheme (System Configuration A) and the conventional Pre-FFT AAA scheme (System Configuration B) are subjects for comparisons. More particularly, several DBF algorithms for each configuration are included, such as MRC, AMBF and SMI. Varieties of multipath channel conditions are conducted to verify the operation of the AAA-SDC scheme and are discussed in next subsections.

4.1 Multipath Channel Condition 1

In this simulation, multipath channel condition is realized to verify the AAA-SDC scheme. Table 3 shows the specification of this simulation condition. It is worthwhile noting that in this condition delay spreads are shorter than GI duration. Therefore, it can be considered as a free ISI channel condition.

Figure 12 shows the BER performances of the AAA-SDC scheme versus SNR with Doppler shift of 0 Hz. The performances of different DBF algorithms on the same system configuration are rather identical. Moreover, the BER

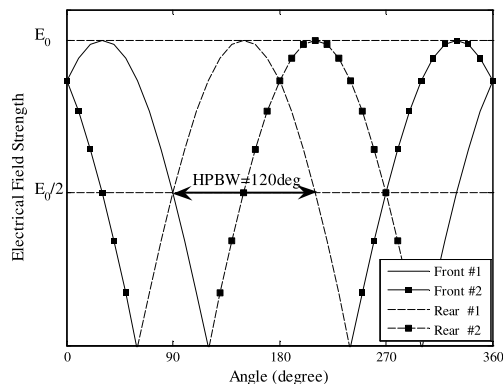


Fig. 11 Allocation of antenna elements in automobile and their directional characteristics.

Table 3 Multipath channel condition 1.

Paths	θ (deg)	DUR (dB)	Delay
#1	0	3	$0.5 * (T_g/8)$
#2	30	0	0
#3	90	3	$3.2 * (T_g/8)$
#4	150	3	$2.5 * (T_g/8)$
#5	210	0	$0.3 * (T_g/8)$
#6	300	3	$4.0 * (T_g/8)$

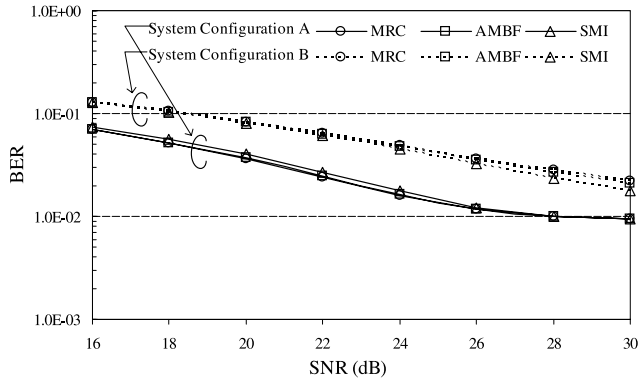


Fig. 12 BER vs. SNR with Doppler shift of 0 Hz.

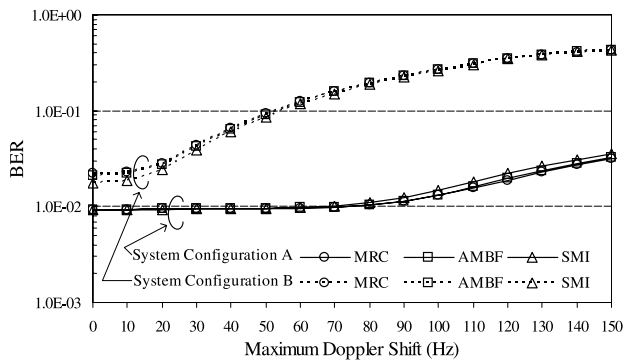


Fig. 13 BER vs. Doppler shift with SNR=30 dB.

performances of System Configuration A outperform those of System Configuration B due to the superiority of the Post-FFT SDC scheme.

In addition, the BER performances of the AAA-SDC scheme versus the maximum Doppler shift with SNR of 30 dB are shown in Fig. 13. Again, the BER performances of different DBF algorithms are similar for each particular system configuration. Interestingly, the DBF algorithms on System Configuration A is seemingly stable in a region of very high Doppler shift because of the perfect frequency error compensation. However, the performances of DBF algorithms on System Configuration B are greatly degraded as Doppler shift increases. As antenna elements in the front and in the rear gather incoming signals with different AOAs, their received signals suffer greatly different Doppler shift, from the front ones to the rear ones, due to their different directional characteristics. As a result, Doppler shift is rarely compensated by the common frequency error compensation and therefore greatly degrades the performances on System Configuration B in a region of high Doppler shift.

4.2 Multipath Channel Condition 2

The channel condition for this simulation is given in Table 4. In this condition, there are two paths with delay spread exceeding GI duration, considered as ISIs, coming from both the front direction and the back direction. Once again, the performances of DBF algorithms on System Configuration

Table 4 Multipath channel condition 2.

Paths	θ (deg)	DUR (dB)	Delay
#1	0	3	$10.0 * (T_g/8)$
#2	30	0	0
#3	90	3	$3.2 * (T_g/8)$
#4	150	3	$11.2 * (T_g/8)$
#5	210	0	$0.3 * (T_g/8)$
#6	300	3	$4.0 * (T_g/8)$

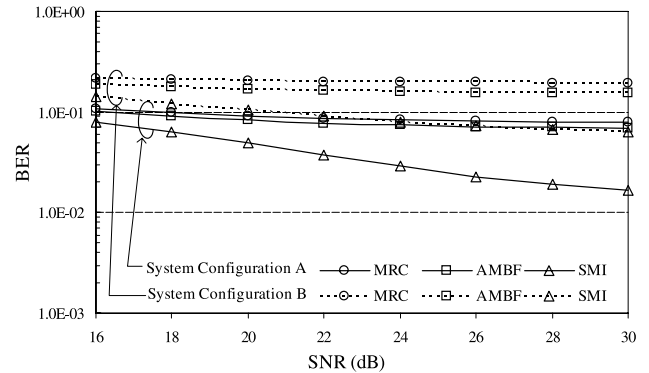


Fig. 14 BER vs. SNR with Doppler shift of 0 Hz.

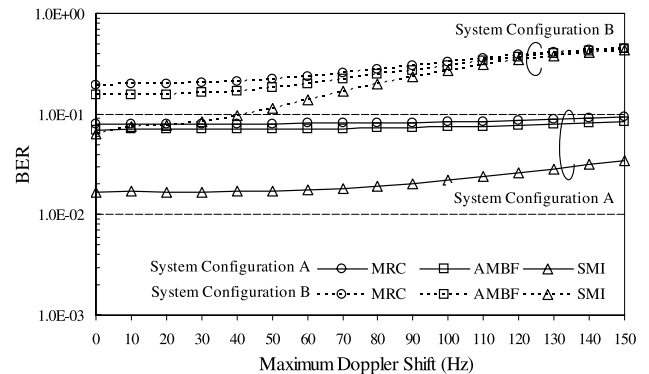


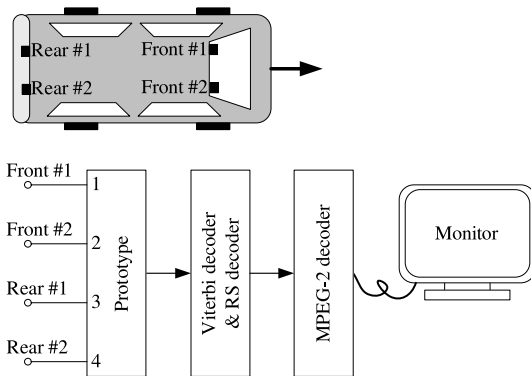
Fig. 15 BER vs. Doppler shift with SNR=30 dB.

A and B are evaluated. Figure 14 shows the BER performances versus SNR in case Doppler shift of 0 Hz. With the presence of interferences, System Configuration A still outperforms System Configuration B. In detail, SMI algorithm on both configurations achieves the best performance due to its ability of suppressing interferences. Let it keep in mind that AMBF algorithm is the improvement of MRC algorithm as discussed in Sect. 2.1. Therefore it is also interesting to note that the performances of AMBF algorithm outperform those of MRC algorithm on both configurations.

BER performances versus Doppler shift in the case of SNR of 30 dB are given in Fig. 15. Similarly, the performances of DBF algorithms on System Configuration A are more stable in a region of high Doppler shift, meanwhile their performances on System Configuration B are severely degraded by Doppler shift. Over all, SMI algorithm achieves the highest performance on both configurations.

Table 5 Experimental conditions.

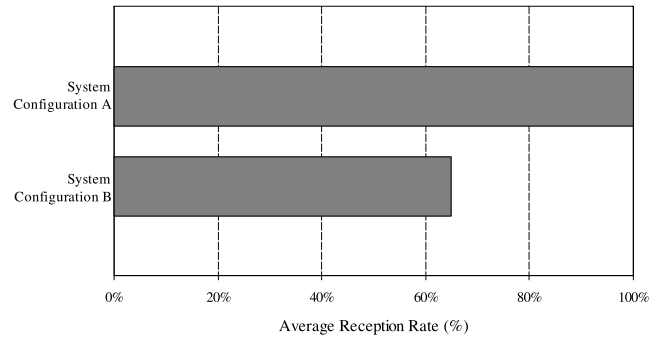
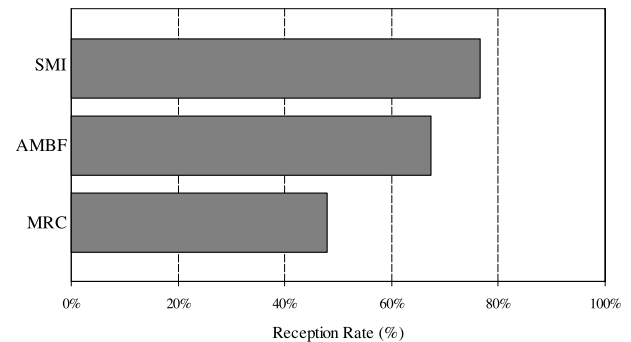
Test Course	City Center Loop Expressway (NLOS environment)	
	Course length	10 km
	Distance to ISDB-T tower	approx. 20 km
Evaluation Conditions	4 on-glass antenna elements	
	Evaluation signal	12-segment HDTV
	Moving speed	80 km/h
	Evaluation period	approx. 8 minutes

**Fig. 16** Illustration of experiment setup.

5. Experimental Results

The prototype of the AAA-SDC scheme is successfully implemented and is the subject of several experiments. The experimental conditions are summarized in Table 5 and the experiment setup is illustrated in Fig. 16. In [17], the directional characteristics of on-glass antennas mounted in different positions in the body of automobile are illustrated. In our experiment setup, four on-glass antenna elements are set in body of automobile, two antenna elements are mounted in corners of the front windshield, whereas the others are mounted in the rear windshield of the experimental automobile. Output signal of the prototype is error-corrected by Viterbi decoder and Reed-Solomon decoder to obtain MPEG-2 stream. The broadcasted signal is then displayed in a monitor to evaluate the reception quality — see Fig. 16.

To validate the reception quality of the prototype, we define the reception rate as the ratio of error-free reception duration to the total experiment duration. In the experiment, the reception rate of the prototype is measured while the experimental vehicle is moving with speed of about 80 km/h in the highway. In the test course, the prototype experiences no co-channel interference, however non-line-of-sight (NLOS) multipath condition with relatively long delay paths is mostly observed during the experiments. The performances of both system configurations, in which MRC, AMBF and SMI are selected, are measured separately. Figure 17 shows the average reception rate of System Configuration A and System Configuration B. In the test course, System Configuration A that utilizes MRC, AMBF and SMI, can achieve the average reception rate of 100%;

**Fig. 17** Performances of system configuration A and B.**Fig. 18** Performances of DBF algorithms in system configuration B.

whereas the average reception rate of System Configuration B utilizing MRC, AMBF and SMI can only reaches up to 65%. Obviously, the performance of mobile ISDB-T receiver set in the high-speed automobile are drastically improved by using the proposed AAA-SDC scheme.

Figure 18 illustrates the performances of MRC, AMBF and SMI in System Configuration B in detail. By exploiting the periodic property of OFDM signal as explained in Sect. 2, the reception rate of AMBF is improved compared with that of MRC. More interestingly, as the receiver experiences mostly NLOS multipath condition with relatively long delay paths in the test course, due to the null steering capability, the performance of SMI outperforms that of MRC and AMBF.

The experimental results are also disclosed in [12] and [18].

6. Conclusions

In circumstances that multiple antenna elements are set in the body of automobile, it is inappropriate to consider their directional characteristics as omnidirectional characteristics. Indeed, the directional characteristics of the front ones focus to the front direction while those of the rear ones focus to the back direction of the automobile.

In this paper, the AAA-SDC scheme is proposed and implemented to improve the performance of mobile ISDB-T receiver in such application. By exploiting the joint software-hardware approach, several DBF algorithms can be supported. Moreover, this approach also provides the

platform in which several system configurations can be reconfigurable on the fly. Simulations and experiments are conducted to verify the performance of the proposed AAA-SDC scheme. The results show that a performance of mobile ISDB-T receiver is drastically improved as the specific directional characteristics of antenna elements are taken into account. The experiment results show that the proposed AAA-SDC scheme achieves the outstanding reception rate up to 100%, meanwhile the reception rate of the Pre-FFT AAA scheme only reaches up to 65%.

Acknowledgments

The authors would like to thank Dr. Shuji Murakami, Kazuhiro Kamiyama and Hiroyuki Mizutani of Magna Design Net Inc. for invaluable contribution to implement the prototype. The authors would like to thank Prof. Nobuyuki Kikuma of Nagoya Institute of Technology for useful discussion and cooperation to enhance the performance of the prototype. Finally, the authors would like to express our gratitude to Associate Prof. Mitoshi Fujimoto of University of Fukui for antenna-related technical discussions.

References

- [1] J.A.C. Bingham, "Multicarrier modulation for data transmission: An idea whose time has come," *IEEE Commun. Mag.*, vol.28, no.5, pp.5–14, May 1990.
- [2] R. Van Nee and R. Prasad, *OFDM for Wireless Multimedia Communication*, pp.39–42, Artech House, 2000.
- [3] N. Kikuma and M. Fujimoto, "Adaptive antennas," *IEICE Trans. Commun.*, vol.E86-B, no.3, pp.968–979, March 2003.
- [4] L.C. Godara, "Application of antenna arrays to mobile communication, Part II: Beam-forming and direction-of-arrival considerations," *Proc. IEEE*, vol.85, no.8, pp.1195–1245, Aug. 1997.
- [5] S. Hara, A. Nishikawa, and Y. Hara, "A novel OFDM adaptive antenna array for delayed signal and Doppler-shifted signal suppression," *Proc. IEEE ICC2001*, vol.7, pp.2302–2306, 2001.
- [6] J. Imai, M. Fujimoto, T. Shibata, N. Itoh, N. Suzuki, and K. Mizutani, "Experimental results of diversity reception for terrestrial digital broadcasting," *IEICE Trans. Commun.*, vol.E85-B, no.11, pp.2527–2530, Nov. 2002.
- [7] S. Sakaguchi, M. Hori, T. Wada, and N. Itoh, "An adaptive array direction control LSI for mobile digital HDTV receivers," Session 7.4: Acquisition System, *IEEE ICCE2005*, USA, Jan. 2005.
- [8] S. Hori, N. Kikuma, and N. Inagaki, "MMSE adaptive array utilizing guard interval in the OFDM systems," *Electron. Commun. Jpn.*, vol.86, no.10, pp.1–9, 2003.
- [9] S. Hori, N. Kikuma, T. Wada, and M. Fujimoto, "Experimental study on array beam forming utilizing the guard interval in OFDM," WD3-3, *International Symposium on Antennas and Propagation ISAP2005*, pp.257–260, Korea, Aug. 2005.
- [10] S. Hori, *Research on Adaptive Array Antenna for OFDM Transmission*, Doctor Dissertation, Nagoya Institute of Technology, Japan, April 2006.
- [11] H. Asato, T. Tabata, D.H. Pham, H. Mizutani, K. Kamiyama, S. Hori, and T. Wada, "A software-configurable adaptive array antenna systems for ISDB-T reception," Session: 11.2 Signal Processing for Multiple Ant., *DVB-T and DAPSK/DMT*, *IEEE Int. Conf. on Consumer Electronics ICCE2006*, USA, Jan. 2006.
- [12] D.H. Pham, T. Tabata, H. Asato, S. Hori, and T. Wada, "Joint hardware-software implementation of adaptive array antenna for ISDB-T reception," *IEICE Trans. Commun.*, vol.E89-B, no.12, pp.3215–3224, Dec. 2006.
- [13] M. Fujimoto, K. Nishikawa, T. Shibata, N. Kikuma, and N. Inagaki, "A novel adaptive array utilizing frequency characteristics of multi-carrier signals," *IEICE Trans. Commun.*, vol.E83-B, no.2, pp.371–379, Feb. 2000.
- [14] S. Nakahara, H. Hamazumi, K. Shibuya, and M. Sasaki, "An application of diversity combination techniques to broadcasting wave relay station for ISDB-T," *ITE Technical Report*, vol.25, no.31, pp.7–12, March 2001.
- [15] K. Higuchi and H. Sasaoka, "Adaptive array suppressing inter-symbol interference based on frequency spectrum in OFDM system," *IEICE Trans. Commun. (Japanese Edition)*, vol.J87-B, no.9, pp.1222–1229, Sept. 2004.
- [16] M. Fujimoto and T. Hori, "Effect of antenna element characteristics on antenna pattern control of array antenna," *IEICE Technical Report*, RCS2004-177, Oct. 2004.
- [17] S. Matsuzawa, K. Sata, and K. Nishikawa, "Study of on-glass mobile antennas for digital terrestrial television," *IEICE Trans. Commun.*, vol.E88-B, no.7, pp.3094–3096, July 2005.
- [18] T. Tabata, H. Asato, D.H. Pham, M. Fujimoto, H. Kikuma, S. Hori, and T. Wada, "Experiment study on adaptive array antenna system for ISDB-T high speed mobile reception," Session 150.5: Smart Ant. Sys., *IEEE Ant. and Propagation Society Int. Symposium (APS2007)*, pp.1697–1700, Hawaii, USA, June 2007.
- [19] M. Speth, F. Classen, and H. Meyr, "Frame synchronization of OFDM systems in frequency selective fading channels," *Proc. Vehicular Tech. Conf. (VTC'97 USA)*, pp.1807–1811, 1997.
- [20] M. Speth, S.A. Fechtel, G. Fock, and H. Meyr, "Optimum receiver design for wireless broad-band systems using OFDM—Part I," *IEEE Trans. Commun.*, vol.47, no.11, pp.1668–1677, Nov. 1999.
- [21] M. Speth, S.A. Fechtel, G. Fock, and H. Meyr, "Optimum receiver design for wireless broad-band systems using OFDM—Part II: A case study," *IEEE Trans. Commun.*, vol.49, no.4, pp.571–578, April 2001.
- [22] F.M. Gardner, "Interpolation in digital modems—Part I: Fundamentals," *IEEE Trans. Commun.*, vol.41, no.3, pp.501–507, March 1993.
- [23] F.M. Gardner, "Interpolation in digital modems—Part I: Implementation and performance," *IEEE Trans. Commun.*, vol.41, no.6, pp.998–1008, June 1993.
- [24] J.G. Proakis, *Digital Communications*, fourth ed., McGraw-Hill, 2001.



Dang Hai Pham was born in Hanoi, Vietnam, on June 7, 1977. He received B.S. degree in Hanoi Univ. of Technology, Vietnam in 2000 and M.S. in Univ. of the Ryukyus, Okinawa, Japan in 2003. Now he is a Ph.D. student in Department of Information Engineering, Univ. of the Ryukyus. His research interests are channel estimation, adaptive array antenna with its application to OFDM.



Jing Gao received his B.E. degree and M.E. degree in Electrical and Electronic Engineering from Ryukyu University, Okinawa, Japan, in 2003 and 2005, respectively. He is currently working toward the Ph.D. degree in Information Engineering at Ryukyu University. His research interests are adaptive array antenna and its application to mobile communications.



Takanobu Tabata was born in Mie, Japan on September 3, 1976. He received B.E. degree in Electrical Engineering from Nagoya Institute of the Technology, Nagoya, Japan, in 2000. He joined Kojima Press Industry Co., Ltd. Aichi, Japan, in 2000. Currently, he is engaged in development of a system for mobile reception of ISDB-T.



Hirokazu Asato was born in Okinawa, Japan on June 20, 1976. He received B.S. degree in Electrical Engineering, Univ. of the Ryukyus, Okinawa, Japan, in 1999. He joined Nihon Synosys Co., Ltd. Tokyo, Japan, in 1999. From 1992 to 2002, he was engaged in technical support of ASIC design. In 2002, he joined Magna Design Net Inc., Okinawa, Japan. Currently, he was engaged in developing and programming related to wireless communication LSI.



Satoshi Hori was born in Aichi, Japan, on November 4, 1964. He received B.E. degree in Electronics and Information Science and Ph.D. from Toyota Technological Institute, Nagoya, Japan, in 1989 and Nagoya Institute of the Technology, Nagoya, Japan, in 2006, respectively. Since he joined Kojima Press Industry Co., Ltd. in 1982, he has been engaged in research and development on antenna systems for automobile use such as adaptive array antenna and vehicle communication. He is a member of

the IEEE.



Tomohisha Wada was born in Hiroshima, Japan, on December 2, 1959. He received B.S. degree in electronic engineering from Osaka Univ., Osaka, Japan, in 1983, M.S.E.E. degree from Stanford Univ., Stanford CA, in 1992, and Ph.D. in electronic engineering from Osaka Univ. in 1994. He joined the ULSI Laboratory, Mitsubishi Electric Corp., Itami, Japan, in 1983. From 1983 to 1999, he has been engaged in the development of CMOS/BiCMOS static RAMs, 3-D graphics controller ASIC, flash memory,

low-voltage static RAM, and synchronous burst static RAMs. In 1998, he joined Mitsubishi Electric Corp., Semiconductor Group, Memory IC Division, Itami, where he has been working on the development of application specific synchronous burst static RAMs. In 1999, he became an Associate Professor with the Department of Information Engineering, Univ. of the Ryukyus, Okinawa, Japan. Since 2001, he has been a Professor at the Department of Information Engineering, Univ. of the Ryukyus, Okinawa, Japan. In 2001, He was the founding member of Magna Design Net, Inc., which is a fab-less LSI design Company for communication related digital signal processing such as OFDM. Currently, he is also the chief scientist of Magna Design Net, Inc. From 1999 up to now, he has been engaged in the research and development of high bandwidth communication systems such as terrestrial video broadcasting receivers and wireless LAN. Currently his research interests include system-level large-scale VLSI design, digital signal processing for high-bandwidth communication, error correction algorithm and circuit, networking software and protocols.